SUPPLEMENTARY MATERIAL

Design of CeO$_2$-supported LaNiO$_3$ perovskites as precursor of highly active catalysts for CO$_2$ methanation

Jon A. Onrubia, [1] B. Pereda-Ayo, [1] José A. González-Marcos, [1] Agustín Bueno-López, [2]

Juan R. González-Velasco[1],*

[1]Department of Chemical Engineering, Faculty of Science and Tecnology, University of the

Basque Country UPV/EHU, Barrio Sarriena, ES48940 Leioa, Bizkaia, Spain

[2] Department of Inorganic Chemistry, University of Alicante, Carretera de San Vicente s/n.

ES03080, Alicante, Spain.

KEYWORDS: CO$_2$ methanation, perovskite, LaNiO$_3$, CeO$_2$ support, Ni nanoparticles
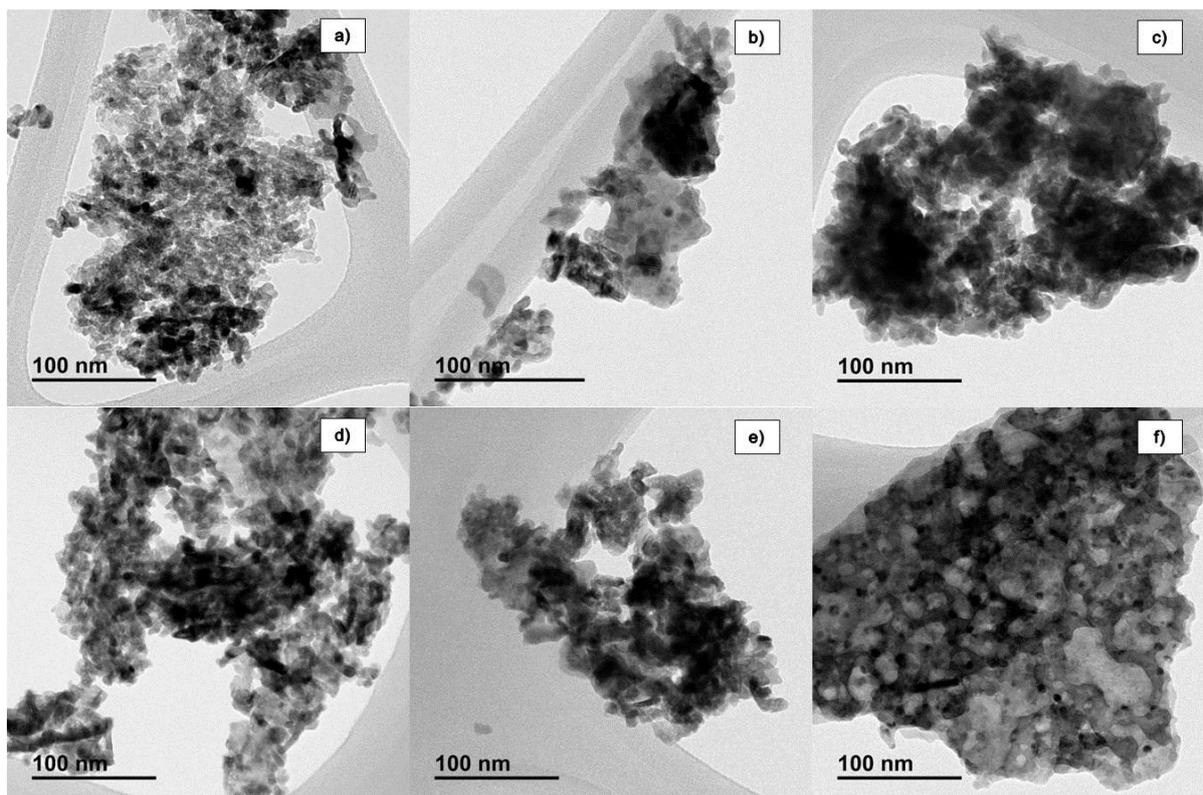
*Corresponding author: juanra.gonzalezvelasco@ehu.es

Figure S1. TEM micrographs of 10% LaNiO$_3$/CeO$_2$, 30% LaNiO$_3$/CeO$_2$ and 50% LaNiO$_3$/CeO$_2$ fresh (a, b, c) and used (d, e, f), respectively.

TEM images of the 10, 30 and 50% LaNiO$_3$/CeO$_2$ catalysts were acquired before (Figures S1a-c) and after reduction + reaction (Figures S1d-f). Two differentiated zones can be observed for fresh samples. On the one hand, ceria phase with small crystals (light grey) homogeneously distributed in all analyzed area. On the other hand, perovskite rich areas (dark grey) supported over ceria can be also identified, especially for high perovskite loading. As can be observed, impregnating ceria with increasing perovskite content increases the particle sizes of perovskite from 10-15 nm to 30-50 nm. Thus, higher LaNiO$_3$ loading promotes perovskite agglomeration, with a more homogeneous particle size.

Regarding TEM images of used samples (Figures S2d-f), a homogeneous distribution of La$_2$O$_3$ phase over ceria support can be identified for all samples. Furthermore, spherical Ni NPs (6-8 nm) can be observed for the 50% LaNiO$_3$/CeO$_2$ sample (Figure S2f), whereas, the higher dispersion and interaction of Ni NPs with the La$_2$O$_3$ and CeO$_2$ phases, limits their identification for 10 and 30% LaNiO$_3$/CeO$_2$ samples.
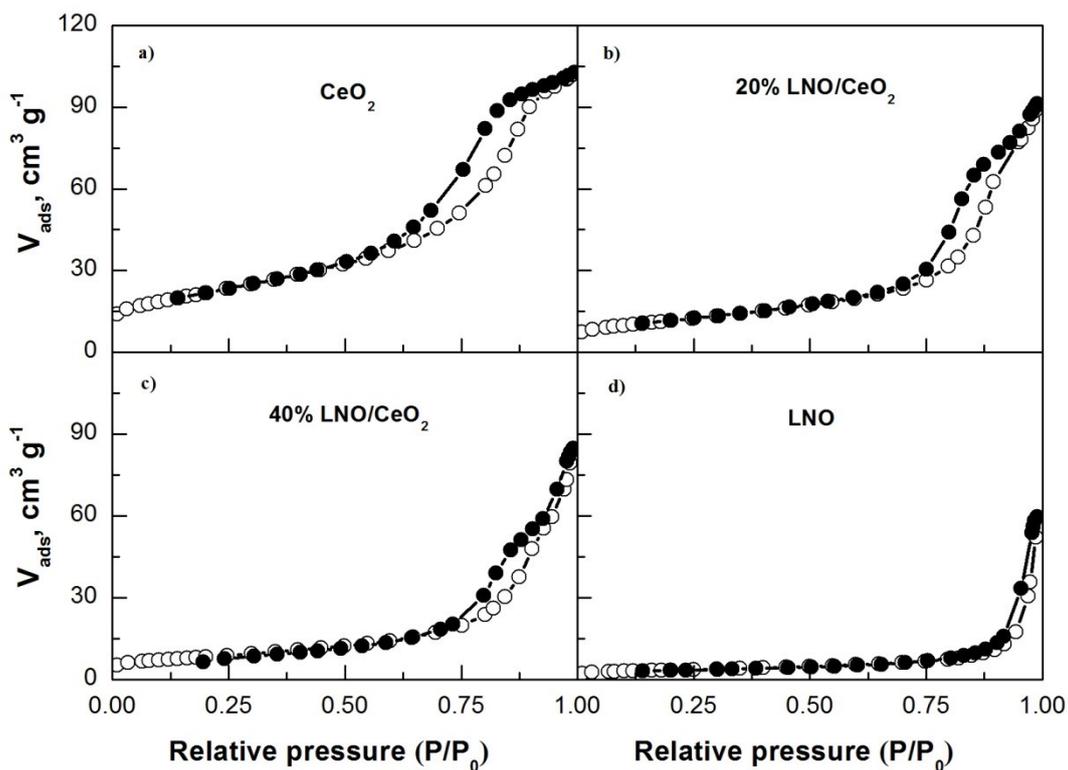
Figure S2. N$_2$-adsorption/desorption isotherms of CeO$_2$ support, and 20% LaNiO$_3$/CeO$_2$, 40% LaNiO$_3$/CeO$_2$ and LaNiO$_3$ samples, after reduction + reaction.

All samples show the IV-type isotherms according to the IUPAC technical classification, which are characteristic of mesoporous materials. In the case of ceria-supported samples, the obtained N$_2$-adsorption/desorption isotherms are intermediate to that obtained for CeO$_2$ support and bulk LaNiO$_3$ perovskite. As the relative pressures (P/P$_0$) vary between 0.70 and 1.0, these materials present H$_2$-type hysteresis loop, implying the relatively narrow pore size distribution of catalysts.
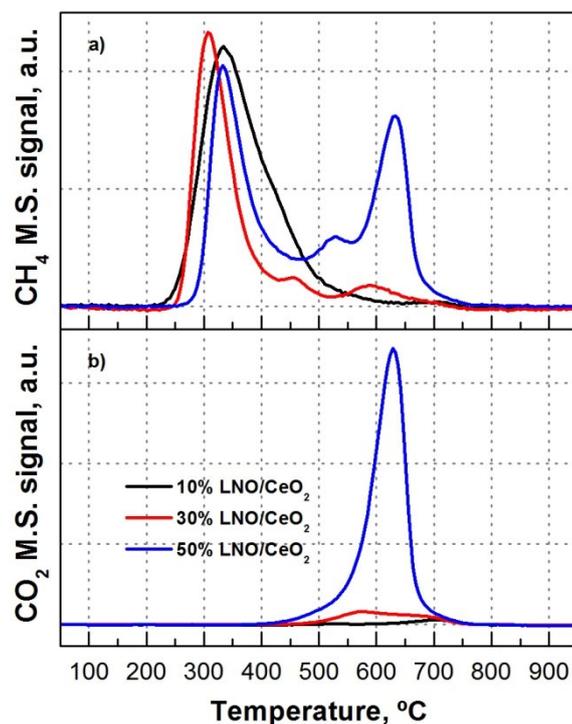
Figure S3. Mass spectrometer signals of: a) CH_4 (m/z = 16) and b) CO_2 (m/z = 44) during H_2-TPR experiments for the 10% LNO/CeO$_2$, 30% LNO/CeO$_2$ and 50% LNO/CeO$_2$ samples.

To gain insight on the hydrogen consumptions centered at 300-325 and 600-625 °C, the H_2-TPR experiments were followed by a mass spectrometer. Figure S3 shows the evolution of CH_4 and CO_2 signals with temperature during H_2-TPR experiments.

The formation of CH_4 is related to the hydrogenation ($CO_2+4H_2 \rightarrow CH_4+H_2O$) of the CO_2 adsorbed in the catalytic surface on Ni^0 sites formed during the H_2-TPR experiment, and as a consequence implies the consumption of additional H_2. This process mainly takes place between 250-550 °C for the 10% LNO/CeO$_2$ sample, whereas an increasing peak is observed at higher temperature for 30% LNO/CeO$_2$ and 50% LNO/CeO$_2$ samples. The high temperature CH_4 formation is accompanied by a CO_2 desorption, formed due to the decomposition of the stronger carbonates adsorbed on the highly agglomerated La_2O_3 on the surface. As expected, an increase of $LaNiO_3$ perovskite loading on ceria support results in a progressive increase of CO_2 desorption peak, due to the higher agglomeration and strength of strong basic sites.
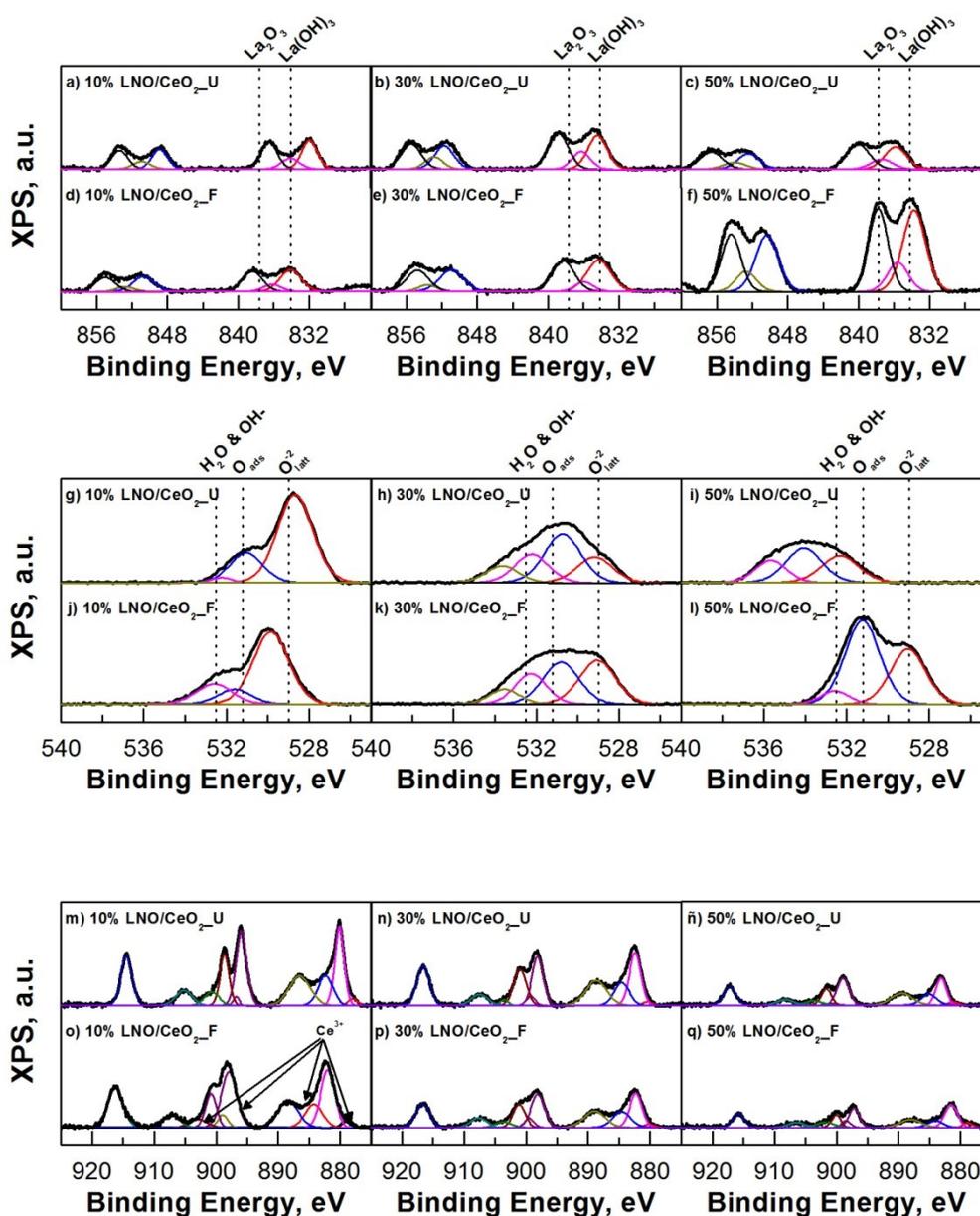
Figure S4. XPS spectra of: a-f) La 3d, g-l) O1s and m-q) Ce 3d transitions. The spectra of fresh (F) 10, 30 and 50% LaNiO$_3$/CeO$_2$ samples are included in the first row, whereas in the second row are included the spectra of the same samples after reduction and CO$_2$ methanation reaction (U).

La 3d$_{5/2}$ transition was deconvoluted in two different contributions located at 834.1 and 837.7 eV with their corresponding shake up satellites (848-856 eV). These contributions were assigned to La^{3+} accommodated within the perovskite lattice and segregated lanthanum as an oxide (La$_2$O$_3$) for the fresh (first row) and used (second row) samples, respectively.

O 1s transition shows a broad emission line between 526 eV and 536 eV, which can be deconvoluted into three distinct peaks around 528.8, 531.2 and 534.0 eV. Lower BE value

5

signal corresponds to lattice oxygen bonded to cations in the crystal structure (O^{2-}_{latt}). Intermediate binding energy contribution (O_{ads}) is ascribed to O-C or O=C bonds, as for example in carbonates, oxygen bonded to cations as segregations (La_2O_3) or weakly bonded O_2 (associated with surfaces defects, i.e. surface vacancies). The signal at highest binding energy values is due to water and hydroxyl groups on the surface.[1,2]

Typically, Ce 3d core level spectra show a three lobed envelope at 879-890, 895-910, and at around 916 eV. As widely reported in literature,[3,4] both Ce $3d_{5/2}$ and Ce $3d_{3/2}$ levels present five component v_o, v, v', v'', v''' and u_o, u, u', u'', u''', respectively. In order to estimate the contribution of Ce^{4+} and Ce^{3+}, the XPS spectra of the x% $LaNiO_3/CeO_2$ catalysts were studied. Since the features characteristic of the Ce^{3+} states derives from the contribution of u_o, v_o, v' and u', the following equation was used to estimate the cerium oxide stoichiometry:

$$Ce^{3+}(\%) = \frac{uo + vo + v' + u'}{\sum(u + v)} \qquad (S.1)$$

referred to all states,[5] using this method the fitted peak areas in the XPS spectra were employed.
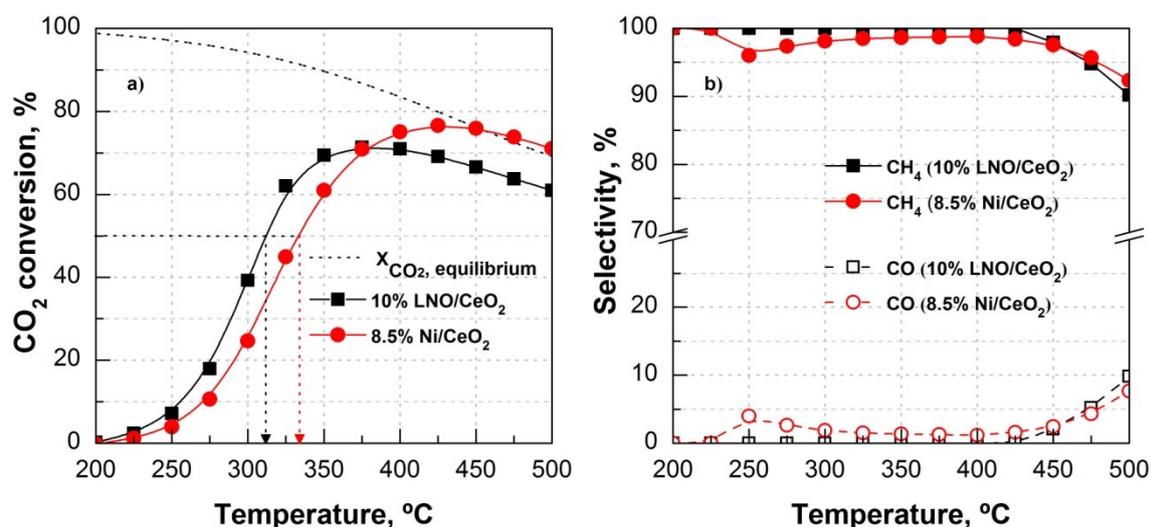
Figure S5. Evolution of: a) CO_2 conversion and b) selectivity towards CH_4 (solid symbols) and CO (open symbols) with reaction temperature for 10% $LaNiO_3/CeO_2$ and 8.5% Ni/CeO_2 catalysts.

Figure S5 compares the evolution of CO_2 conversion and the selectivity towards methane and carbon monoxide as a function of the reaction temperature for 10% $LaNiO_3/CeO_2$ and 8.5% Ni/CeO_2 catalysts. Note that the later formulation was one of the most active catalysts reported in the literature for the CO_2 methanation application.[6,7] As can be observed, the catalyst obtained from the 10% $LaNiO_3/CeO_2$ precursor is more active than the reference sample developed in our previous study at low and intermediates temperatures. In fact, the temperature at which 50% CO_2 conversion is obtained (T_{50}) is reduced from 334 °C to 312 °C for 8.5% Ni/CeO_2 and 10% $LaNiO_3/CeO_2$ catalysts, respectively. CH_4 is the main reaction product in both cases, with selectivity above the 90% in the whole range of temperatures analyzed. However, the selectivity to CH_4 is 100% for the catalyst developed in this study below 425 ºC, whereas is slightly lower for the 8.5% Ni/CeO_2 catalyst. Thus, the catalytic material obtained after the controlled reduction of the 10% $LaNiO_3/CeO_2$ precursor shows higher CO_2 to CH_4 conversion than 8.5% Ni/CeO_2 model catalyst. These results remark that the novel materials developed in this study can be considered as promising catalysts for CO_2 methanation.

References

1 S. Mickevičius, S. Grebinskij, V. Bondarenka, B. Vengalis, K. Šliužienė, B.A. Orlowski, V. Osinniy and W. Drube, *J. Alloys Comp.*, 2006, **423**, 107.

2 G. Pantaleo, V. La Parola, F. Deganello, P. Calatozzo, R. Bal and A.M. Venezia, *Appl. Catal. B: Environ.*, 2015, **164**, 135.

3 F. Le Normand, J. El Fallah, L. Hilaire, P. Légaré, A. Kotani, J.C. Parlebas, *Solid State Commun.*, 1989, **71**, 885.

4 A. Pfau, K.D. Schierbaum, *Surf. Sci.*, 1994, **321**, 71.

5 J. El Fallah, L. Hilaire, M. Roméo, F. Le Normand, *J. Electron. Spectrosc.,* 1995, **73**, 89.

6 S. Tada, T. Shimizu, H. Kameyama, T. Haneda and R. Kikuchi, *Int. J. Hydrogen Energy*, 2012, **37**, 5527.

7 A. Cárdenas-Arenas, A. Quindimil, A. Davó-Quiñonero, E. Bailón-García, D. Lozano-Castelló, U. De-La-Torre, B. Pereda-Ayo, J.A. González-Marcos, J.R. González-Velasco, A. Bueno-López, *Appl. Mater. Today,* 2020, **19**, 100591.